

TAPS: Task-Agnostic Policy Sequencing

Christopher Agia*, Toki Migimatsu*, Jiajun Wu, Jeannette Bohg

Abstract— Advances in robotic skill acquisition have made it possible to build general-purpose libraries of primitive skills for downstream manipulation tasks. However, naively executing these learned primitives one after the other is unlikely to succeed without accounting for dependencies between actions prevalent in long-horizon plans. We present Task-Agnostic Policy Sequencing (TAPS), a scalable framework for training manipulation primitives and coordinating their geometric dependencies at plan-time to efficiently solve long-horizon tasks never seen by any primitive during training. Based on the notion that Q-functions encode a measure of action feasibility, we formulate motion planning as a maximization problem over the expected success of each individual primitive in the plan, which we estimate by the product of their Q-values. Our experiments indicate that this objective function approximates ground truth plan feasibility and, when used as a planning objective, reduces myopic behavior and thereby promotes task success. We further demonstrate how TAPS can be used for task and motion planning by estimating the geometric feasibility of candidate action sequences provided by a task planner. We evaluate our approach in simulation and on a real robot.

I. INTRODUCTION

Performing sequential manipulation tasks requires a robot to reason about dependencies between actions. Consider the example in Fig. 1, where the robot needs to grab an object outside its workspace by first using an L-shaped hook to pull the target object closer. How the robot picks up the hook affects whether the target object will be reachable.

Traditionally, planning actions to ensure the geometric feasibility of a sequential manipulation task is handled by motion planning [1–3] which typically requires privileged knowledge about the environment state and its dynamics. Learning-based approaches [4–6] can acquire primitive skills without requiring this privileged information. However, using learned primitives to perform sequential manipulation tasks is an unsolved problem. While myopically executing learned primitives one after another may solve a small subset of sequential manipulation tasks, solving more complex tasks requires planning with these primitives to ensure the geometric feasibility of the entire sequence.

Prior work focuses on sequencing learned primitives at *train time* to solve a single [7] or a small set of long-horizon tasks [8]. Such methods are limited when facing arbitrary long-horizon tasks, since they need to be trained on all the possible long-horizon tasks or primitive sequences they might encounter at test time. In our framework, we assume that a task planner provides us with a sequence of abstract primitives at *test time* that will then be grounded with

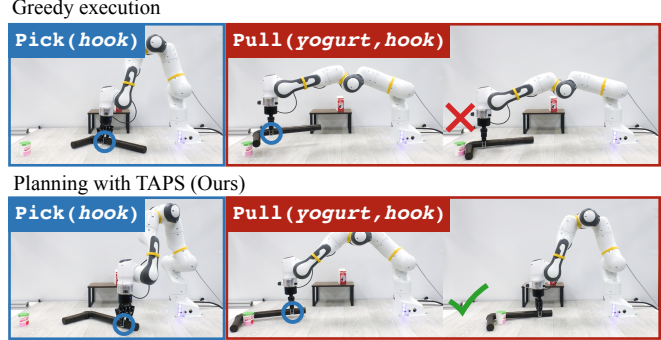


Fig. 1: Sequential manipulation tasks often contain geometric dependencies between actions. In this example, the robot needs to use the hook to pull the block into its kinematic workspace so it is close enough to pick up. The top row shows how greedy execution of primitives results in the robot myopically picking up the hook in a way that prevents it from reaching the block. We present a method for planning with primitives to maximize long-horizon success without the need to train the primitives on long-horizon tasks.

concrete actions by sequencing learned primitives. This makes our method *task-agnostic*, since we can sequence primitives to solve long-horizon tasks not seen at train time.

The key insight of our method, *Task-Agnostic Policy Sequencing* (TAPS), is that geometric preconditions of learned primitives are implicitly encoded by Q-functions that model the expected success of the primitive given the current state and action. We use off-the-shelf RL algorithms to acquire Q-functions, and then define a planning objective to maximize all the Q-functions in the primitive sequence to ensure their feasibility. Evaluating downstream Q-functions on future states requires learning a dynamics model that can forward predict future states. We also use uncertainty quantification (UQ) to avoid visiting states and planning actions that are out-of-distribution (OOD) for the learned primitives. We train all of these components independently per primitive, making it easy to gradually expand a library of primitives without the need to retrain existing ones.

Our contributions are three-fold: we propose 1) a framework to train an extensible library of task-agnostic primitives, 2) a planning method to sequence primitives towards arbitrary long-horizon tasks, and 3) a method to solve Task and Motion Planning (TAMP) problems with learned primitives. In extensive experiments, we demonstrate that TAPS outperforms baselines for solving long-horizon tasks with complex geometric dependencies between actions. We also demonstrate that our framework works on a real robot.

II. RELATED WORK

A. Primitive skill learning

How to represent and acquire composable primitive skills is a widely studied problem in robotics. A broad class

*Authors contributed equally to this work.

The authors are with Stanford University, Stanford, CA 94305, USA.
Toyota Research Institute provided funds to support this work.

of methods uses Learning from Demonstration (LfD) [5]. Dynamic Movement Primitives (DMPs) [9–11] are a form of LfD that learns the parameters of dynamical systems encoding movements [12–15]. More recent extensions integrate DMPs with deep neural networks to learn more flexible policies [16, 17]; for instance, to acquire a large library of skill policies from human video demonstrations [18]. Skill discovery methods instead identify action patterns in offline datasets [19] and either distill them into policies [20, 21] or extract skill priors for use in downstream tasks [22, 23]. Primitive skills can also be acquired via trial-and-error with Reinforcement Learning (RL) [24–28] and offline RL [29].

An advantage of our planning framework is that it is agnostic to the types of primitives employed, requiring only that it is possible to predict the probability of the skill’s success given the current state and skill parameter (action). Here, we learn policies over parameterized action primitives [30] which can express a range of manipulation skills with a handful of skill parameters, empowering the search for feasible parameter values with motion planning.

B. Long-horizon robot planning

Once primitive skills have been acquired, using them to perform sequential manipulation tasks remains an open challenge. [31, 32] propose data-driven methods to determine the *symbolic* feasibility of primitives and only control their timing, while we seek to ensure the *geometric* feasibility of primitives by controlling their trajectories. Other techniques rely on task planning [33, 34], subgoal planning [35], or meta-adaptation [36, 37] to guide the sequencing of learned primitives to novel long-horizon goals. However, the tasks considered in these works do not feature rich geometric dependencies between actions that necessitate motion planning.

The options framework [38] and parameterized action MDPs [39] outline *control* paradigms that train a high-level policy to engage low-level policies [40, 41] or primitives [7, 42, 43] towards a goal. [44] proposes a hierarchical RL method that uses the value functions of lower-level policies as the state space for a higher-level RL policy. Our work is also related to model-based RL methods which jointly learn dynamics and reward models to guide planning [45–47], policy search [48, 49], or combine both [50, 51]. While these methods demonstrate that policy hierarchies and model-based planning can enable RL to solve long-horizon problems, they are typically trained in the context of a single task. In contrast, we seek to *plan* with lower-level primitives policies to solve tasks never seen before.

Closest in spirit to our work is that of Xu et al. [8], Deep Affordance Foresight (DAF), which proposes to learn a dynamics model, skill-centric affordances (i.e. value functions), and a skill proposal network that serves as a higher-level RL policy. We identify several drawbacks with DAF: first, because DAF relies on multi-task experience for training, generalizing to tasks outside the distribution of training tasks may be difficult; second, the dynamics, affordance models, and skill proposal need to be trained synchronously, making scalability an issue when training a large library of

primitives; third, their planner samples actions from uniform random distributions, which prevents it from scaling to high-dimensional action spaces and long horizons. We are unique in that our dynamics, skill policies, and affordances (Q-functions) are learned independently per primitive, and then without additional training, we combine them at planning time to solve arbitrary long-horizon tasks. We compare our method against DAF in the planning experiments.

C. Task and motion planning

TAMP solves problems that require a combination of symbolic and geometric reasoning [2, 52]. DAF learns a skill proposal network to replace the typical task planner in TAMP, akin to [53]. Another prominent line of research learns components of the TAMP system, often from a dataset of precomputed solutions [54–58]. The problems considered in our paper involve complex geometric dependencies between actions that are typical in TAMP. However, TAPS only performs the geometric reasoning part and by itself is not a TAMP method. We demonstrate in experiments that it can be effectively combined with symbolic planners to solve TAMP problems.

III. PROBLEM SETUP

Our goal is to solve long-horizon manipulation tasks that require sequential execution of primitive policies from a library $\mathcal{L} = \{\pi^k, \dots, \pi^K\}$. Each primitive k is associated with a contextual bandit, or a single timestep Markov Decision Process (MDP)

$$\mathcal{M}^k = (\mathcal{S}^k, \mathcal{A}^k, T^k, R^k, \rho^k), \quad (1)$$

where \mathcal{S}^k is the state space, \mathcal{A}^k is the action space, $T^k(s'^k | s^k, a^k)$ is the transition model, $R^k(s^k, a^k)$ is the binary reward function, and $\rho^k(s^k)$ is the initial state distribution.

A long-horizon domain is one in which each timestep involves the execution of one primitive. Upon executing a primitive action a^k , the state evolves according to the primitive transition dynamics $T^k(s'^k | s^k, a^k)$. A long-horizon domain is specified by the tuple

$$\overline{\mathcal{M}} = \left(\mathcal{M}^{1:K}, \overline{\mathcal{S}}, \overline{T}^{1:K}, \overline{\rho}^{1:K}, \Psi^{1:K} \right), \quad (2)$$

where $\mathcal{M}^{1:K}$ is the set of MDPs whose primitives can be executed in the long-horizon domain, $\overline{\mathcal{S}}$ is the state space of the long-horizon domain, $\overline{T}^k(\overline{s}' | \overline{s}, a^k)$ is an extension of primitive dynamics $T^k(s'^k | s^k, a^k)$ that models how the entire long-horizon state evolves with action a^k , $\overline{\rho}^k(\overline{s})$ is an extension of primitive initial state distributions $\rho^k(s^k)$ over the long-horizon state space, and $\Psi^k : \overline{\mathcal{S}} \rightarrow \mathcal{S}^k$ is a function that maps from the long-horizon state space to the state space of primitive k . We assume that the dynamics $T^k(s'^k | s^k, a^k)$, $\overline{T}^k(\overline{s}' | \overline{s}, a^k)$ and initial state distributions $\rho^k(s^k)$, $\overline{\rho}^k(\overline{s}^k)$ are unknown for all primitives k .

Note that while the primitives may have different state spaces \mathcal{S}^k , they must all be obtainable from the long-horizon state space $\overline{\mathcal{S}}$ via Ψ^k . This is to ensure that the primitives can be used together in the same environment to perform

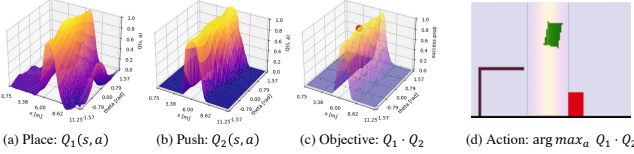


Fig. 2: Planning in a 2D toy domain where the agent needs to get the green block under the brown receptacle with two primitives: Place() and Push() that operate on the horizontal position x of the green block. Plots (a) and (b) show the value functions across (x, θ) for each primitive. Place() is only trained to get the green block on the ground, so the planner must determine $a = x$ s.t. Push() is unobstructed. To maximize the probability of long-horizon task success (Eq. 7), we want to find an action that maximizes the product of Q-functions, as shown in plot (c).

long-horizon tasks. Upon observing a state $\bar{s} \in \bar{\mathcal{S}}$ in the sequential environment, we can obtain the primitive state via $s^k = \Psi^k(\bar{s})$. In the simplest case, all the state spaces are identical, and Ψ^k is simply the identity function. Another case is that \bar{s} is constructed as the concatenation of all $s^{1:K}$, and $\Psi^k(\bar{s})$ extracts the slice in \bar{s} corresponding to s^k .

IV. TASK-AGNOSTIC POLICY SEQUENCING

A. Grounding primitive sequences with action plans

We assume we are given a plan skeleton of primitives $\tau = [\pi_1, \dots, \pi_H] \in \mathcal{L}^H$ that should be executed sequentially to solve a long-horizon task. Let \mathcal{M}_h with subscript h denote the primitive MDP corresponding to the h -th primitive in the sequence (in contrast to \mathcal{M}^k with superscript k , which denotes the k -th primitive MDP in the primitive library). A long-horizon task is considered successful if every primitive reward r_1, \dots, r_H received during execution is 1.

Given an initial state $\bar{s} \in \bar{\mathcal{S}}$, our problem is to ground the plan skeleton τ with an action plan $\xi = [a_1, \dots, a_H] \in \mathcal{A}_1 \times \dots \times \mathcal{A}_H$ that maximizes the probability of succeeding at the long-horizon task. This is framed as the optimization problem $\arg \max_{a_{1:H}} J$, where the maximization objective J is the task success probability

$$J(a_{1:H}; \bar{s}_1) = p(r_1 = 1, \dots, r_H = 1 \mid \bar{s}_1, a_{1:H}). \quad (3)$$

$r_{1:H}$ are the primitive rewards received at each timestep.

By the Markov assumption, rewards are conditionally independent given states and actions. We can express the probability of task success as the product of reward probabilities

$$J(a_{1:H}; \bar{s}_1) = \prod_{h=1}^H p(r_h = 1 \mid \bar{s}_1, a_{1:h}). \quad (4)$$

With the long-horizon dynamics model $\bar{T}^k(\bar{s}' \mid \bar{s}, a^k)$, the objective can be cast as the expectation

$$J = \mathbb{E}_{\bar{s}_{2:H} \sim \bar{T}_{1:H-1}} [\prod_{h=1}^H p(r_h = 1 \mid \bar{s}_h, a_h)]. \quad (5)$$

Because the primitive rewards are binary, the primitive success probabilities are equivalent to Q-values:

$$p(r_h \mid \bar{s}_h, a_h) = \mathbb{E}[r_h \mid \bar{s}_h, a_h] = Q_h(\Psi_h(\bar{s}_h), a_h). \quad (6)$$

The objective is finally expressed in terms of Q-values:

$$J = \mathbb{E}_{\bar{s}_{2:H} \sim \bar{T}_{1:H-1}} [\prod_{h=1}^H Q_h(\Psi_h(\bar{s}_h), a_h)]. \quad (7)$$

This planning objective is simply the product of Q-values evaluated along the trajectory $(\bar{s}_1, a_1, \dots, \bar{s}_H, a_H)$, where the states are predicted by the long-horizon dynamics

model: $\bar{s}_2 = \bar{T}_1(\bar{s}_1, a_1), \dots, \bar{s}_H = \bar{T}_{H-1}(\bar{s}_{H-1}, a_{H-1})$.¹ Optimizing this objective requires access to Q-functions $Q^k(s^k, a^k)$ and dynamics models $\bar{T}^k(\bar{s}, a^k)$. In Sec. V, we propose a training procedure for learning these models.

B. Ensuring action plan feasibility

A plan skeleton $\tau = \pi_{1:H}$ is feasible only if, for every pair of consecutive primitives i and j , there is a non-zero overlap between the terminal state distribution of i and the initial state distribution of j . More formally,

$$\mathbb{E}_{\bar{s}_i \sim \bar{\rho}_i, a_i \sim \mathcal{A}_i, \bar{s}_j \sim \bar{\rho}_j} [\bar{T}_i(\bar{s}_j \mid \bar{s}_i, a_i)] > 0, \quad (8)$$

where $\bar{\rho}_i$ and $\bar{\rho}_j$ are the initial state distributions for primitives i and j , respectively, and a_i is uniformly distributed with respect to action space \mathcal{A}_i for primitive i . Given a state $\bar{s}_i \sim \bar{\rho}_i$, it is part of the planner's job to determine an action a_i that produces a valid subsequent state $\bar{s}_j \sim \bar{\rho}_j$ if one exists. Failing to do so constitutes an OOD event for primitive j where the subsequent state \bar{s}_j has drifted beyond the region of the state space where $Q_j(\Psi_j(\bar{s}_j), a_j)$ is well-defined and π_j is executable.

Neglecting state distributional shift over an action plan ξ may degrade the quality of objective function J with spuriously high Q-values. Moreover, Eq. 8 cannot be explicitly computed to determine the validity of actions because the initial state distributions of all primitives $\bar{\rho}^k(\bar{s}^k)$ are unknown. We can detect OOD states (and actions) by performing uncertainty quantification (UQ) on the Q-functions $Q^k(s^k, a^k)$. Filtering out Q-values with high uncertainty would result in action plans ξ that are robust (have low uncertainty) while maximizing the task feasibility objective. We discuss efficient methods for training UQ models on learned Q-functions in Sec. V-C.

V. TRAINING PRIMITIVES

A. Policies

One of the key advantages of our approach is that the primitive policies can be trained individually, and then composed together at test time to solve unseen sequential tasks. For each primitive, we want to obtain a policy $\pi^k : \mathcal{S}^k \rightarrow \mathcal{A}^k$ that can solve the primitive-specific task specified by its MDP \mathcal{M}^k . In addition to the policy, we also want to learn a Q-function for each primitive:

$$Q^k(s^k, a^k) = \mathbb{E}_{s'^k \sim T^k(\cdot \mid s^k, a^k)} [R^k(s^k, a^k)]. \quad (9)$$

Our framework is agnostic to the method for acquiring the policy and Q-function. Many deep RL algorithms are able to learn the policy (actor) and Q-function (critic) simultaneously with unknown dynamics [59, 60]. We therefore leverage off-the-shelf RL algorithms to learn a

¹One might consider maximizing the *sum* of Q-values instead of the product, but this may not reflect the probability of task success. For example, if we want to optimize a sequence of ten primitives, consider a plan that results in nine Q-values of 1 and one Q-value of 0, for a total sum of 9. One Q-value of 0 would indicate just one primitive failure, but this is enough to cause a failure for the entire task. Compare this to a plan with ten Q-values of 0.9. This plan has an equivalent sum of 9, but it is preferable because it has a non-zero probability of succeeding.

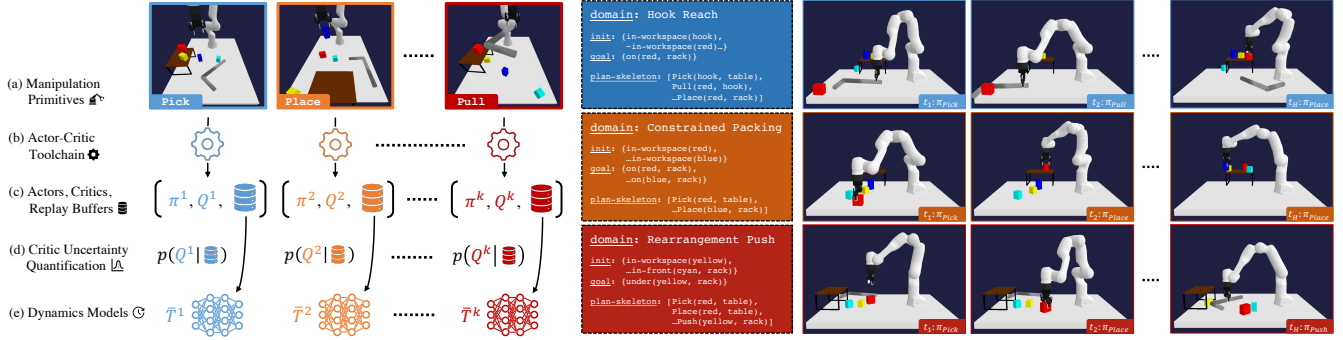


Fig. 3: **Left:** Training pipeline. We train each primitive independently on single-step environments with primitive-specific rewards. We use the experience collected by each primitive to train (1) a SCOD model to predict OOD critic inputs and (2) a dynamics model per primitive. The benefit of training each primitive independently is that we can easily add primitives to the library or even mix policy acquisition strategies (e.g. RL and handcrafted policies). Our planning framework ensures that the primitives can be composed to perform any long-horizon task even if they weren't trained to perform those tasks. **Right:** Example evaluation tasks. We evaluate our method on 9 tasks: 3 Hook Reach tasks, where the robot needs to use the hook to bring objects closer, 3 Constrained Packing tasks, where the robot needs to place blocks on the rack, and 3 Rearrangement Push tasks, where the robot needs to remove obstacles to push a target block under the rack. The 9 tasks contain a range of geometric complexity and plan skeleton lengths.

policy and Q-function for each primitive. For other methods, policy evaluation can always be performed to obtain a Q-function after a policy has been learned. For our experiments, we specifically use Soft Actor-Critic (SAC) [61].

B. Dynamics

The dynamics models are used to predict future states at which each downstream Q-function in the plan will be evaluated. We learn a deterministic model for each primitive k :

$$\bar{s}' = \bar{T}^k(\bar{s}, a^k). \quad (10)$$

Using the forward prediction loss, each dynamics model is trained on the state transition experience (\bar{s}, a^k, \bar{s}') collected during policy training for primitive k :

$$L_{\text{dynamics}}(\bar{T}^k; \bar{s}, a^k, \bar{s}') = \left\| \bar{T}^k(\bar{s}, a^k) - \bar{s}' \right\|_2^2. \quad (11)$$

C. Uncertainty quantification

Measuring the epistemic uncertainty over the Q-values will allow us to identify when dynamics-predicted states and planned actions drift OOD for downstream primitive critics Q^k . We leverage recent advances in neural network UQ, taking an approximate Bayesian computational approach to obtain an explicit Gaussian posterior distribution over Q-values

$$p(Q^k | s^k, a^k, \mathcal{D}^k, w^k) = \mathcal{N}(\mu_{Q^k}, \sigma_{Q^k}; w^k) \quad (12)$$

with sketching curvature for OOD detection (SCOD) [62]. We apply SCOD to obtain the weights w^k from which the posterior distributions over each critic Q^j are derived. The advantages of SCOD over common UQ techniques [63, 64] are that it imposes no train-time dependencies on any algorithms used in our framework, and it requires only the experience $(\bar{s}, a^k) \sim \mathcal{D}^k$ collected over the course of training primitive policies π^k .

VI. PLANNING WITH PRIMITIVES

A. Planning action sequences

To find action sequences that maximize the probability of long-horizon task success (Eq. 7), we use sampling-based methods: shooting and cross entropy method (CEM) [65].

In shooting, we simply sample action plans $\xi = a_{1:H} \in \mathcal{A}_1 \times \dots \times \mathcal{A}_H$, and choose the one with the highest predicted objective score. CEM is an extension of shooting, where the action sampling distribution is iteratively refined to fit a fraction of the population with the highest objective scores. With small action spaces and short primitive sequences, randomly sampling action plans from a uniform distribution may often be sufficient. However, this strategy suffers from the curse of dimensionality and does not scale to the large action spaces and long primitive sequences that we consider. Meanwhile, directly sequencing actions $a^k \sim \pi^k(s^k)$ from the primitive policies learned via off-the-shelf RL methods (V-A) produces myopic plans that rarely succeed for tasks with complex geometric dependencies between actions.

The policies can be leveraged to initialize a sampling-based search with an action plan that is likely to be closer to an optimal plan than one sampled uniformly at random. We therefore use two variants of shooting and CEM, termed policy shooting and policy CEM, which sample actions from Gaussian distributions $a^k \sim \mathcal{N}(\pi^k(s^k), \sigma)$, where the mean is the action predicted by the policy and the standard deviation is a planning hyperparameter.

B. Task and motion planning

In Sec. IV-A, we start with the assumption that the plan skeleton $\tau = \pi_{1:H}$ is given, although our approach is agnostic to where it comes from. For example, the plan skeletons can be computed by symbolic planners in a TAMP loop, invoking our planner to evaluate the geometric feasibility of proposed plans. We can describe TAMP domains by combining the Planning Domain Description Language (PDDL) [66] with the long-horizon domain \mathcal{M} in Eq. 2:

$$\mathcal{D}_{\text{TAMP}} = (\Phi, \Pi^{1:H}, \mathcal{M}). \quad (13)$$

Φ is the set of predicates that describe binary-valued symbolic properties of objects, and $\Pi^{1:H}$ are the symbolic actions, one per primitive, with symbolic pre-conditions and effects that describe how each primitive modifies the symbolic state of the world. A TAMP problem is specified by the tuple

$$\mathcal{P}_{\text{TAMP}} = (\mathcal{O}, \mathbf{g}, \mathbf{s}_1, \bar{s}_1), \quad (14)$$

where \mathcal{O} is the set of symbolic objects in the problem, \mathbf{g} is the symbolic goal specified as a first-order logic formula, \mathbf{s}_1 is the initial symbolic state represented as a set of propositions (predicates instantiated by object arguments), and $\overline{\mathbf{s}}_1 \in \overline{\mathcal{S}}$ is the initial state for $\overline{\mathcal{M}}$.

Given a TAMP problem, the task planner will solve the PDDL problem $(\mathcal{O}, \mathbf{g}, \mathbf{s}_1)$ to produce a candidate plan skeleton $\tau = \pi_{1:H}$. We then perform motion planning as described in VI-A to find a feasible action plan $\xi = a_{1:H}$ for the candidate plan skeleton. The task planner continues to find the next candidate plan skeleton. After some termination criterion is met, we return the candidate plan skeleton and grounded action plan with the highest probability of task success (Eq. 7).

VII. EXPERIMENTS

In our experiments, we test the following hypotheses:

- H1** Maximizing the product of learned Q-functions (Eq. 7) translates to maximizing long-horizon task success.
- H2** Primitives trained with our framework are able to generalize to unseen long-horizon tasks.
- H3** Our planning method can be combined with a task planner to solve TAMP problems.

We evaluate our method on a 3D manipulation domain with 4 primitives: $\text{Pick}(a, b)$: pick a from b ; $\text{Place}(a, b)$: place a onto b ; $\text{Pull}(a, \text{hook})$: pull a into the robot's workspace with a *hook*; and $\text{Push}(a, \text{hook})$: push a with a *hook*.

The state space $\overline{\mathcal{S}}$ is a sequence of low-dimensional object states that contains information such as 6D poses. The primitive state spaces \mathcal{S}^k are constructed so that the first m object states correspond to the m arguments of the corresponding primitive. For example, a state for $\text{Pick}(box, rack)$ will contain first the *box*'s state, then the *rack*'s state, followed by a random permutation of the remaining object states.

The primitive action spaces \mathcal{A}^k in this domain are all 4D. For example, an action for $\text{Pick}(a, b)$ specifies the 3D grasp position of the end-effector relative to the target a and orientation about the world z -axis.

Our evaluation is on 9 different long-horizon tasks (i.e. plan skeletons τ) in this domain (Fig. 3). The tasks cover a range of symbolic and geometric complexity, with plan skeleton lengths ranging from 4 to 10 actions. Each task involves geometric dependencies between actions, which motivate the need for planning. For each task, we use 100 randomly generated instances (i.e. object configurations) for evaluation.

A. Product of Q-functions approximates task success (H1)

We evaluate **H1** by comparing it to an **Oracle** baseline that runs forward simulations with policy shooting to find plans that achieve ground-truth task success. Our method, on the other hand, uses learned Q-functions and dynamics to predict task success as the product of Q-functions. We expect that planning with this objective will come close to matching the task success upper bound provided by **Oracle**.

We compare several planning methods: **Policy Shooting** and **Policy CEM**, which use the learned policies to bias the action sampling distributions (VI-A), as well as **Random Shooting** and **Random CEM**, which use uniform action

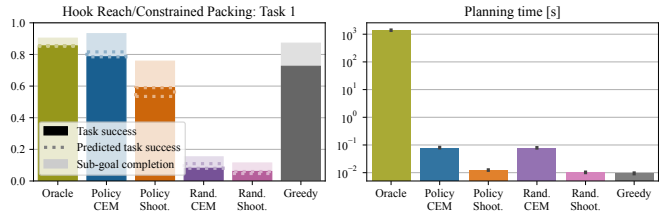


Fig. 4: A small-scale experiment comparing how well our method performs to **Oracle** planning. The left shows the average success rates across the two domains (Hook Reach and Constrained Packing). The dark bars indicate the ground truth task success, and the light bars indicate sub-goal completion rate, which measures how close the plan was to successfully completing the task. The predicted task success computed from the product of Q-values is indicated by a dotted line. Our method with **Policy CEM** is able to nearly match the success rate of **Oracle** while taking 4 orders of magnitude less time, as shown on the right side.

priors. We also compare with **Greedy**, which does not plan but greedily executes the policies. The evaluation metrics are ground truth task success, sub-goal completion rate (what percentage of actions in a plan are successfully executed), and predicted task success computed from Eq. 7.

Due to the significant amount of time required to run forward simulations for **Oracle**, we limit the number of samples evaluated during planning to 1000 for all methods. This is not enough to succeed at the most complex tasks, so in our evaluation, we only use the easiest task from the Hook Reach and Constrained Packing domains.

The results from both tasks are averaged and presented in Fig. 4. **Oracle** achieves the highest success rate, as expected, but is not perfect likely because 1000 samples are not enough to solve the tasks. **Policy CEM** nearly matches **Oracle**'s success rate, which demonstrates that maximizing the product of Q-functions is a good proxy for maximizing task success. **Policy CEM** also exhibits a low success prediction error, which demonstrates that the learned Q-functions and dynamics generalize well to these unseen long-horizon tasks. Meanwhile, planning with these learned models runs 4 orders of magnitude faster than **Oracle** and does not require ground truth knowledge about the environment state or dynamics.

Policy Shooting performs slightly worse than **Policy CEM**, which indicates CEM's strength in finding local maxima. **Random CEM** and **Random Shooting** perform quite poorly, indicating that the planning space is too large (16D for these tasks) for random sampling. **Greedy** performs strongly, perhaps indicating that these simple tasks from the two domains may be doable without planning.

B. TAPS primitives generalize to long-horizon tasks (H2)

In this experiment, we specifically test the ability of our framework to solve 9 long-horizon tasks with geometric dependencies between actions. We compare against DAF [8], a state-of-the-art method for learning to solve TAMP problems. While DAF employs a skill proposal network that serves the role of a task planner, task planning is outside the scope of this paper, so we leave out skill proposal from this evaluation and compare only against the skills trained with DAF (**DAF-Skills**), which are comprised of dynamics and affordance models. DAF's planning objective is similar to ours, except they evaluate the product

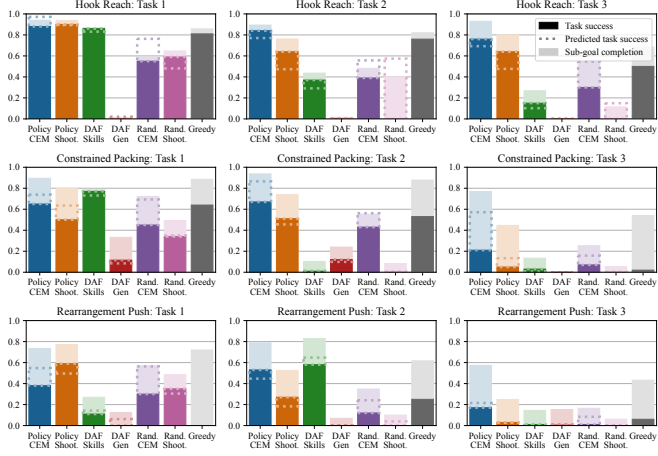


Fig. 5: Planning experiment with 3 domains, each with 3 tasks. Our method with **Policy CEM** outperforms **DAF-Skills**, which is trained directly on the evaluation task, for all tasks but two. Our method is able to generalize to all of these tasks without ever seeing them during training. **DAF-Gen** shows the generalization performance of the **DAF-Skills** models when evaluated on unseen tasks within the same domain.

of affordances rather than Q-functions. We give **DAF-Skills** the same plan skeleton τ that is given to our method. We also augment DAF’s shooting planner with CEM.

Like other model-based RL methods, DAF requires training on a set of long-horizon tasks that is representative of the evaluation task distribution. We therefore train one **DAF-Skills** model per task (9 total) and run our evaluation on the same task. We also test the ability of these models to generalize to the other two tasks within the same domain (**DAF-Gen**). For the simplest tasks, we expect **DAF-Skills** to perform at least as well as our method, if not better, since it is trained on the same task used for evaluation. For the longer horizon tasks, it may perform worse, since the probability of completing a task drops exponentially with the length of the task, which means **DAF-Skills** will naturally get fewer chances to explore later steps. We train **DAF-Skills** and our method for 48 hours each, and allow up to 100,000 samples per dimension for planning.

The results are presented in Fig. 5. Our method with Policy CEM achieves the highest success rate for most tasks. DAF’s performance is inconsistent; while it achieves competitive success rates for 3 out of 9 tasks, it gets relatively low success on the others. This indicates that training the model directly on the long-horizon task may not be the most effective strategy. Our method of training each policy on primitive-specific environments and then generalizing to long-horizon tasks via planning is efficient from a training perspective, since the same trained primitives can be used for all tasks, and also scales better to longer horizons.

C. TAPS can be integrated into a TAMP framework (H3)

In this experiment, we combine our framework with a PDDL task planner as described in VI-B and evaluate it on two TAMP problems. In **Hook Reach**, the robot needs to decide the best way to pick up a block, which may or may not be in its workspace. In **Constrained Packing**, the robot needs to place a fixed number of objects on the rack

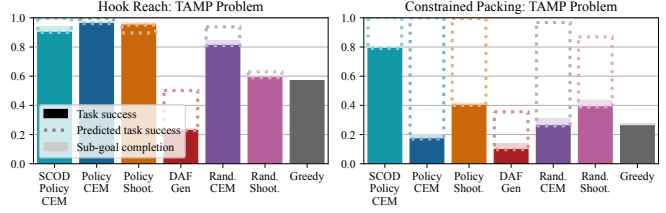


Fig. 6: Integration of our planning framework with task planning to solve TAMP problems. The poor performance of the methods without SCOD in the **Constrained Packing** problem highlights the potential importance of UQ for TAMP problems.

but is free to choose among any of the objects on the table. To mimic what the robot might find in an unstructured, real-world environment, some of these objects are distractor objects that are initialized in ways not seen by the primitives during training (e.g. the blocks can be stacked, placed behind the base, or tipped over). The task planner may end up selecting these distractor objects for placing on the rack, but since the policies have not been trained to handle these objects, their predicted success may be unreliable. UQ is particularly important for such scenarios, so we introduce **SCOD Policy CEM**, which filters out candidate plans with high uncertainty in the predicted task success.

The results are presented in Fig. 6. **Policy CEM** achieves 97% success for the **Hook Reach** TAMP problem. **SCOD Policy CEM** suffers a slight performance drop. However, for **Constrained Packing**, which contains OOD states, **SCOD Policy CEM** strongly outperforms the other methods. Exploring different ways to integrate UQ into our planning framework is a promising direction for future work.

D. Real world sequential manipulation

We demonstrate that policies trained with our framework can be used to perform sequential manipulation tasks in a real robot environment. We take RGB-D images from a Kinect v2 camera and use manually tuned color thresholds to segment the objects. With these segmentations, we estimate object poses using the depth image, which is then used to construct the initial environment state \bar{s}_1 . Qualitative results are provided in the supplementary video.

VIII. CONCLUSION

We present a framework for sequencing task-agnostic policies that have been trained independently. The key to generalization is planning actions that maximize the probability of long-horizon task success, which we model using the product of learned Q-values. This requires learning a dynamics model to predict future states and using UQ to filter out OOD states that the primitives do not support. The result is a library of primitives that can be composed to solve arbitrary long-horizon tasks with complex geometric dependencies between actions. Future work includes investigating methods to handle high-dimensional observations, combining the library of learned primitives with a set of handcrafted primitives, and exploring planning objectives that seek to optimize trajectories, beyond finding geometrically feasible trajectories.

REFERENCES

[1] S. M. LaValle, *Planning Algorithms*. Cambridge University Press, 2006.

[2] M. Toussaint, “Logic-geometric programming: An optimization-based approach to combined task and motion planning,” in *Twenty-Fourth International Joint Conference on Artificial Intelligence*, 2015.

[3] M. Toussaint, K. Allen, K. Smith, and J. B. Tenenbaum, “Differentiable physics and stable modes for tool-use and manipulation planning,” in *Proceedings of Robotics: Science and Systems*, Pittsburgh, Pennsylvania, June 2018.

[4] L. Kaelbling, M. Littman, and A. Moore, “Reinforcement learning: A survey,” *Journal of Artificial Intelligence Research*, vol. 4, pp. 237–285, 1996.

[5] B. D. Argall, S. Chernova, M. Veloso, and B. Browning, “A survey of robot learning from demonstration,” *Robotics and autonomous systems*, vol. 57, no. 5, pp. 469–483, 2009.

[6] S. Schaal, “Is imitation learning the route to humanoid robots?” *Trends in Cognitive Sciences*, vol. 3, no. 6, pp. 233–242, 1999.

[7] M. Dalal, D. Pathak, and R. R. Salakhutdinov, “Accelerating robotic reinforcement learning via parameterized action primitives,” *Advances in Neural Information Processing Systems*, vol. 34, pp. 21 847–21 859, 2021.

[8] D. Xu, A. Mandlekar, R. Martín-Martín, Y. Zhu, S. Savarese, and L. Fei-Fei, “Deep affordance foresight: Planning through what can be done in the future,” in *2021 IEEE International Conference on Robotics and Automation (ICRA)*. IEEE, 2021, pp. 6206–6213.

[9] S. Schaal, “Dynamic movement primitives-a framework for motor control in humans and humanoid robotics,” in *Adaptive motion of animals and machines*. Springer, 2006, pp. 261–280.

[10] P. Pastor, H. Hoffmann, T. Asfour, and S. Schaal, “Learning and generalization of motor skills by learning from demonstration,” in *2009 IEEE International Conference on Robotics and Automation*. IEEE, 2009, pp. 763–768.

[11] S. M. Khansari-Zadeh and A. Billard, “Learning stable nonlinear dynamical systems with gaussian mixture models,” *IEEE Transactions on Robotics*, vol. 27, no. 5, pp. 943–957, 2011.

[12] A. J. Ijspeert, J. Nakanishi, and S. Schaal, “Movement imitation with nonlinear dynamical systems in humanoid robots,” in *Proceedings 2002 IEEE International Conference on Robotics and Automation (Cat. No. 02CH37292)*, vol. 2. IEEE, 2002, pp. 1398–1403.

[13] T. Matsubara, S.-H. Hyon, and J. Morimoto, “Learning stylistic dynamic movement primitives from multiple demonstrations,” in *2010 IEEE/RSJ International Conference on Intelligent Robots and Systems*. IEEE, 2010, pp. 1277–1283.

[14] A. Ude, A. Gams, T. Asfour, and J. Morimoto, “Task-specific generalization of discrete and periodic dynamic movement primitives,” *IEEE Transactions on Robotics*, vol. 26, no. 5, pp. 800–815, 2010.

[15] T. Kulyicius, K. Ning, M. Tamosiunaite, and F. Wörötter, “Joining movement sequences: Modified dynamic movement primitives for robotics applications exemplified on handwriting,” *IEEE Transactions on Robotics*, vol. 28, no. 1, pp. 145–157, 2011.

[16] S. Bahl, M. Mukadam, A. Gupta, and D. Pathak, “Neural dynamic policies for end-to-end sensorimotor learning,” *Advances in Neural Information Processing Systems*, vol. 33, pp. 5058–5069, 2020.

[17] S. Bahl, A. Gupta, and D. Pathak, “Hierarchical neural dynamic policies,” *arXiv preprint arXiv:2107.05627*, 2021.

[18] L. Shao, T. Migimatsu, Q. Zhang, K. Yang, and J. Bohg, “Concept2robot: Learning manipulation concepts from instructions and human demonstrations,” *The International Journal of Robotics Research*, vol. 40, no. 12-14, pp. 1419–1434, 2021.

[19] T. Shankar, S. Tulsiani, L. Pinto, and A. Gupta, “Discovering motor programs by recomposing demonstrations,” in *International Conference on Learning Representations*, 2019.

[20] T. Shankar and A. Gupta, “Learning robot skills with temporal variational inference,” in *International Conference on Machine Learning*. PMLR, 2020, pp. 8624–8633.

[21] A. Ajay, A. Kumar, P. Agrawal, S. Levine, and O. Nachum, “Opal: Offline primitive discovery for accelerating offline reinforcement learning,” *arXiv preprint arXiv:2010.13611*, 2020.

[22] A. Singh, H. Liu, G. Zhou, A. Yu, N. Rhinehart, and S. Levine, “Parrot: Data-driven behavioral priors for reinforcement learning,” *arXiv preprint arXiv:2011.10024*, 2020.

[23] K. Pertsch, Y. Lee, and J. J. Lim, “Accelerating reinforcement learning with learned skill priors,” *arXiv preprint arXiv:2010.11944*, 2020.

[24] A. Rajeswaran, V. Kumar, A. Gupta, G. Vezzani, J. Schulman, E. Todorov, and S. Levine, “Learning complex dexterous manipulation with deep reinforcement learning and demonstrations,” *arXiv preprint arXiv:1709.10087*, 2017.

[25] D. Kalashnikov, A. Irpan, P. Pastor, J. Ibarz, A. Herzog, E. Jang, D. Quillen, E. Holly, M. Kalakrishnan, V. Vanhoucke *et al.*, “Scalable deep reinforcement learning for vision-based robotic manipulation,” in *Conference on Robot Learning*. PMLR, 2018, pp. 651–673.

[26] D. Kalashnikov, J. Varley, Y. Chebotar, B. Swanson, R. Jonschkowski, C. Finn, S. Levine, and K. Hausman, “Mt-opt: Continuous multi-task robotic reinforcement learning at scale,” *arXiv preprint arXiv:2104.08212*, 2021.

[27] A. Sharma, S. Gu, S. Levine, V. Kumar, and K. Hausman, “Dynamics-aware unsupervised discovery of skills,” *arXiv preprint arXiv:1907.01657*, 2019.

[28] Y. Lu, K. Hausman, Y. Chebotar, M. Yan, E. Jang, A. Herzog, T. Xiao, A. Irpan, M. Khansari, D. Kalashnikov *et al.*, “Aw-opt: Learning robotic skills with imitation and reinforcement at scale,” in *Conference on Robot Learning*. PMLR, 2022, pp. 1078–1088.

[29] Y. Chebotar, K. Hausman, Y. Lu, T. Xiao, D. Kalashnikov, J. Varley, A. Irpan, B. Eysenbach, R. Julian, C. Finn *et al.*, “Actionable models: Unsupervised offline reinforcement learning of robotic skills,” *arXiv preprint arXiv:2104.07749*, 2021.

[30] B. Da Silva, G. Konidaris, and A. Barto, “Learning parameterized skills,” *arXiv preprint arXiv:1206.6398*, 2012.

[31] D. Kappler, P. Pastor, M. Kalakrishnan, M. Wüthrich, and S. Schaal, “Data-driven online decision making for autonomous manipulation,” in *Robotics: science and systems*, vol. 11, 2015.

[32] T. Migimatsu, W. Lian, J. Bohg, and S. Schaal, “Symbolic state estimation with predicates for contact-rich manipulation tasks,” in *IEEE International Conference on Robotics and Automation (ICRA)*. IEEE, 2022.

[33] B. Wu, S. Nair, L. Fei-Fei, and C. Finn, “Example-driven model-based reinforcement learning for solving long-horizon visuomotor tasks,” *arXiv preprint arXiv:2109.10312*, 2021.

[34] D.-A. Huang, D. Xu, Y. Zhu, A. Garg, S. Savarese, L. Fei-Fei, and J. C. Niebles, “Continuous relaxation of symbolic planner for one-shot imitation learning,” in *2019 IEEE/RSJ International Conference on Intelligent Robots and Systems (IROS)*. IEEE, 2019, pp. 2635–2642.

[35] A. Simeonov, Y. Du, B. Kim, F. R. Hogan, J. Tenenbaum, P. Agrawal, and A. Rodriguez, “A long horizon planning framework for manipulating rigid pointcloud objects,” *arXiv preprint arXiv:2011.08177*, 2020.

[36] D. Xu, S. Nair, Y. Zhu, J. Gao, A. Garg, L. Fei-Fei, and S. Savarese, “Neural task programming: Learning to generalize across hierarchical tasks,” in *2018 IEEE International Conference on Robotics and Automation (ICRA)*. IEEE, 2018, pp. 3795–3802.

[37] D.-A. Huang, S. Nair, D. Xu, Y. Zhu, A. Garg, L. Fei-Fei, S. Savarese, and J. C. Niebles, “Neural task graphs: Generalizing to unseen tasks from a single video demonstration,” in *Proceedings of the IEEE/CVF conference on computer vision and pattern recognition*, 2019, pp. 8565–8574.

[38] R. S. Sutton, D. Precup, and S. Singh, “Between mdps and semi-mdps: A framework for temporal abstraction in reinforcement learning,” *Artificial intelligence*, vol. 112, no. 1-2, pp. 181–211, 1999.

[39] W. Masson, P. Ranchod, and G. Konidaris, “Reinforcement learning with parameterized actions,” in *Thirtieth AAAI Conference on Artificial Intelligence*, 2016.

[40] P.-L. Bacon, J. Harb, and D. Precup, “The option-critic architecture,” in *Proceedings of the AAAI Conference on Artificial Intelligence*, vol. 31, no. 1, 2017.

[41] O. Nachum, S. S. Gu, H. Lee, and S. Levine, “Data-efficient hierarchical reinforcement learning,” *Advances in neural information processing systems*, vol. 31, 2018.

[42] S. Nasiriany, H. Liu, and Y. Zhu, “Augmenting reinforcement learning with behavior primitives for diverse manipulation tasks,” in *2022 International Conference on Robotics and Automation (ICRA)*. IEEE, 2022, pp. 7477–7484.

[43] R. Chitnis, S. Tulsiani, S. Gupta, and A. Gupta, “Efficient bimanual manipulation using learned task schemas,” in *2020 IEEE International Conference on Robotics and Automation (ICRA)*. IEEE, 2020, pp. 1149–1155.

[44] D. Shah, P. Xu, Y. Lu, T. Xiao, A. Toshev, S. Levine, and B. Ichter, “Value function spaces: Skill-centric state abstractions for long-horizon reasoning,” *arXiv preprint arXiv:2111.03189*, 2021.

[45] C. Finn and S. Levine, “Deep visual foresight for planning robot motion,” in *2017 IEEE International Conference on Robotics and*

Automation (ICRA). IEEE, 2017, pp. 2786–2793.

[46] K. Chua, R. Calandra, R. McAllister, and S. Levine, “Deep reinforcement learning in a handful of trials using probabilistic dynamics models,” *Advances in neural information processing systems*, vol. 31, 2018.

[47] D. Hafner, T. Lillicrap, I. Fischer, R. Villegas, D. Ha, H. Lee, and J. Davidson, “Learning latent dynamics for planning from pixels,” in *International conference on machine learning*. PMLR, 2019, pp. 2555–2565.

[48] M. Janner, J. Fu, M. Zhang, and S. Levine, “When to trust your model: Model-based policy optimization,” *Advances in Neural Information Processing Systems*, vol. 32, 2019.

[49] D. Hafner, T. Lillicrap, J. Ba, and M. Norouzi, “Dream to control: Learning behaviors by latent imagination,” *arXiv preprint arXiv:1912.01603*, 2019.

[50] K. Xie, H. Bharadhwaj, D. Hafner, A. Garg, and F. Shkurti, “Skill transfer via partially amortized hierarchical planning,” 2020.

[51] R. Sekar, O. Rybkin, K. Daniilidis, P. Abbeel, D. Hafner, and D. Pathak, “Planning to explore via self-supervised world models,” in *International Conference on Machine Learning*. PMLR, 2020, pp. 8583–8592.

[52] C. R. Garrett, T. Lozano-Pérez, and L. P. Kaelbling, “Pddlstream: Integrating symbolic planners and blackbox samplers via optimistic adaptive planning,” in *Proceedings of the International Conference on Automated Planning and Scheduling*, vol. 30, 2020, pp. 440–448.

[53] C. Wang, D. Xu, and L. Fei-Fei, “Generalizable task planning through representation pretraining,” *arXiv preprint arXiv:2205.07993*, 2022.

[54] Z. Wang, C. R. Garrett, L. P. Kaelbling, and T. Lozano-Pérez, “Active model learning and diverse action sampling for task and motion planning,” in *2018 IEEE/RSJ International Conference on Intelligent Robots and Systems (IROS)*. IEEE, 2018, pp. 4107–4114.

[55] D. Driess, J.-S. Ha, and M. Toussaint, “Deep visual reasoning: Learning to predict action sequences for task and motion planning from an initial scene image,” *arXiv preprint arXiv:2006.05398*, 2020.

[56] R. Chitnis, T. Silver, B. Kim, L. P. Kaelbling, and T. Lozano-Perez, “Camps: Learning context-specific abstractions for efficient planning in factored mdps,” *arXiv preprint arXiv:2007.13202*, 2020.

[57] T. Silver, R. Chitnis, A. Curtis, J. B. Tenenbaum, T. Lozano-Perez, and L. P. Kaelbling, “Planning with learned object importance in large problem instances using graph neural networks,” in *Proceedings of the AAAI conference on artificial intelligence*, vol. 35, no. 13, 2021, pp. 11962–11971.

[58] D. Driess, J.-S. Ha, R. Tedrake, and M. Toussaint, “Learning geometric reasoning and control for long-horizon tasks from visual input,” in *2021 IEEE International Conference on Robotics and Automation (ICRA)*. IEEE, 2021, pp. 14298–14305.

[59] T. P. Lillicrap, J. J. Hunt, A. Pritzel, N. Heess, T. Erez, Y. Tassa, D. Silver, and D. Wierstra, “Continuous control with deep reinforcement learning,” *arXiv preprint arXiv:1509.02971*, 2015.

[60] S. Fujimoto, H. Hoof, and D. Meger, “Addressing function approximation error in actor-critic methods,” in *International conference on machine learning*. PMLR, 2018, pp. 1587–1596.

[61] T. Haarnoja, A. Zhou, K. Hartikainen, G. Tucker, S. Ha, J. Tan, V. Kumar, H. Zhu, A. Gupta, P. Abbeel *et al.*, “Soft actor-critic algorithms and applications,” *arXiv preprint arXiv:1812.05905*, 2018.

[62] A. Sharma, N. Azizan, and M. Pavone, “Sketching curvature for efficient out-of-distribution detection for deep neural networks,” in *Uncertainty in Artificial Intelligence*. PMLR, 2021, pp. 1958–1967.

[63] M. Ganaie, M. Hu *et al.*, “Ensemble deep learning: A review,” *arXiv preprint arXiv:2104.02395*, 2021.

[64] Y. Gal and Z. Ghahramani, “Dropout as a bayesian approximation: Representing model uncertainty in deep learning,” in *international conference on machine learning*. PMLR, 2016, pp. 1050–1059.

[65] R. Rubinstein, “The cross-entropy method for combinatorial and continuous optimization,” *Methodology and computing in applied probability*, vol. 1, no. 2, pp. 127–190, 1999.

[66] D. McDermott, M. Ghallab, A. Howe, C. Knoblock, A. Ram, M. Veloso, D. Weld, and D. Wilkins, *PDDL—The Planning Domain Definition Language Version 1.2*, 1998.